



Production and characterization of duplex coatings (HVOF and PVD) on Ti–6Al–4V substrate

E. Bemporad^a, M. Sebastiani^{a,*}, D. De Felicis^a, F. Carassiti^a, R. Valle^b, F. Casadei^b

^a Department of Mechanical and Industrial Engineering, University of "Roma Tre", via della Vasca navale 79, Rome, 00146, Italy

^b Centro Sviluppo Materiali SpA, Surface Engineering and Ceramic Unit Via di Castel Romano 100, Rome, 00128, Italy

Abstract

Present paper deals with modelling, production and characterization of HVOF PVD (WC–Co and TiN or CrN, respectively) duplex coatings deposited on Ti–6Al–4V substrate for application in automotive industry. As a preliminary analysis, an analytical study of the contact stress distribution under spherical indenter in both coated and uncoated systems, and a finite element evaluation of residual stresses were performed: results showed that the presence of an interlayer with intermediate hardness and stiffness (such as the WC–Co coating) plays a fundamental role in the improvement of the load carrying capacity. Starting from the results of simulations, morphological and compositional characterization of the coatings were performed using SEM and AFM techniques. Mechanical properties were investigated by micro indentation techniques and composite hardness modelling; toughness of the system was qualitatively analysed by Rockwell C indentation. Wear rate of the coatings was measured by an implemented rotating wheel method. Results show higher superficial composite hardness, toughness, adhesion and lower wear rate, in comparison with the simple monolayer system.

© 2005 Elsevier B.V. All rights reserved.

Keywords: Duplex systems; PVD; HVOF; Load carrying capacity

1. Introduction

Mechanical resistance of non-ferrous alloy components subject to severe wear conditions strongly depends on the thickness, hardness and stiffness of the surface protective wear resistant layer. Physical Vapour Deposition (PVD) coatings show both very low values for wear rate, friction coefficient and high hardness. Nevertheless PVD techniques allow to obtain just thin coatings ($<10\mu\text{m}$), which do not warrant good mechanical resistance in presence of high contact stresses, during the whole lifetime of component, especially when they are used on softer substrates. Such a limit is currently overcome by utilizing either duplex processes or graded systems, which allow to reach high thickness with mechanical properties optimized gradually from the substrate–coating interface to the outer surface.

Titanium and its alloy are used extensively in aerospace and mechanical application because of the excellent combination of high specific strength, which is maintained at elevated temperature, high resistance to fracture and good corrosion resistance.

Ti–6Al–4V is currently the most widely used of all titanium alloys since it can be heat-treated to different strength levels, it is weldable and relatively easy to machine [2].

On the other hand, titanium alloys often show low hardness, very low load bearing capacity and poor resistance to sliding wear, so that a coating procedure is always necessary in those applications which involve high contact stresses and severe sliding wear [1–3]; PVD coatings are used often to this aim.

Nevertheless, a very thin hard layer on such a soft substrate cannot lead to a mechanically effective structure: differences both in hardness and Young modulus between coating and substrate do not provide a good distribution of contact stresses and abrasive stresses, so that the coated system in some application behaves even worse than the uncoated one [1]. For instance, thin coatings such as TiN deposited by PVD can provide excellent tribological properties in terms of quite low friction coefficient and high resistance to wear, but catastrophic premature failure will occur if the substrate plastically deforms under an high applied load.

In addition to this, titanium alloys often show poor adhesion properties thus requiring expensive surface pre-treatment before deposition [3].

* Corresponding author. Tel.: +39 0655173200; fax: +39 0655173256.

E-mail address: marco.sebastiani@stm.uniroma3.it (M. Sebastiani).

A solution can be represented by duplex systems, obtained by the sequential use of two (or more) coating technologies to have properties which are not obtainable through a single process.

Nowadays the most widely used duplex system for titanium alloys consists of a deep hardened layer obtained by plasma nitriding, on which a thin film is deposited, generally by PVD [22].

Such a system not only provides a harder layer between the soft substrate and the PVD top-layer, but it also does not change the differences in stiffness between the two materials: the load bearing capacity is therefore enhanced, but not completely optimized.

An optimized duplex coating should consist of a harder and also stiffer interlayer, which allows a better distribution of contact stresses, avoiding plastic deformation of the substrate; such a system has not been fully investigated for titanium alloys.

The basic idea of the present work is to produce and characterize a duplex coating for Ti–6Al–4V alloy consisting of a High Velocity Oxygen Fuel (HVOF) thermally sprayed WC–Co thick layer and a TiN (or CrN) thin top-layer.

The aim of this work was to obtain information about how such a system can represent a good material matching in terms of elastic modulus, hardness and coefficient of thermal expansion through thickness variation.

Basing on analytical calculation of contact stresses and finite element simulation of residual stresses, two types of coating were realized, varying the PVD top layer; the mechanical and morphological characterization of coatings was aimed to point out improvement in terms of superficial composite hardness, wear resistance, interface toughness in comparison with the single-layer PVD coating.

2. Experimental details

2.1. Deposition of coatings

Coatings under examination consisted of a duplex system: Ti–6Al–4V substrate was coated first with WC17%Co thick layer by High Velocity Oxygen Fuel technique, then a TiN or CrN thin layer as a top coat was deposited by Cathodic Arc PVD.

Deposition of HVOF coating was performed using a commercial HVOF torch (process parameters shown in Table 1; average thickness of WC–Co coating was of 500 μm , measured by cross-section optical microscope analysis. Microstructure of the coating, porosity and phases distribution were evaluated by image analysis on polished samples.

Polishing of sprayed coating often represents the most problematic phase: the hardness of the coating, its lamellar structure and residual porosity do not allow the use of

Table 1
Process parameters for HVOF deposition

Working distance	Oxygen	Kerosene ratio	Work temperature
380 mm	$16 \cdot 10^{-2} \text{ m}^3/\text{s}$	$7.57 \cdot 10^{-6} \text{ m}^3/\text{s}$	400 °C

Table 2
Sequence of the polishing procedure for the HVOF layer

Lapping film size	30 μm	15 μm	3 μm	1 μm	0.5 μm	0.1 μm
Time (s)	120	60	30	30	20	20
Load applied (N)	20	20	10	10	5	5

traditional polishing procedures to obtain satisfactory results (i.e., proper roughness without surface damage).

In order to prepare the HVOF coating surface for the subsequent deposition of the TiN or CrN layer by PVD, an accurate polishing procedure was set up, by using diamond lapping films from 30 down to 0.1 μm of abrading particles size, and a modified manual grinder was used as sample holder.

The sequence of polishing procedure is reported in Table 2.

The aim of such a procedure was to obtain a polished HVOF surface roughness (R_a) smaller than 0.2 μm , measured using contact profilometer and Atomic Force Microscope (AFM) techniques.

Deposition of PVD coatings was performed using process parameters shown in Table 3; about 3 μm TiN and CrN PVD coating were realized on each HVOF sample having different WC–Co thickness.

In order to have comparative information both PVD coatings were also deposited on uncoated Ti–6Al–4V.

2.2. Analytical calculation of contact stress field

In order to have an evaluation of the load carrying capacity of the coatings under examination, an analytical calculation of the elastic contact stress field was performed, by using a recently developed software package [4]. The code solves the elastic problem of the contact between coated systems and a spherical indenter: the contact stress fields can thus be plotted for every point of the structure.

By imposing values for Young moduli and yield stresses of each layer the code also evaluate the critical load (i.e., that one which causes incipient plastic deformation) for a range of possible values of contact radii. In such a way it is possible to obtain a quantitative comparison between coated and uncoated systems in terms of load bearing capacity.

2.3. Finite element simulation of residual stresses

Residual stresses in PVD coatings [5–7] arise from the contribution and interaction of two main sources: thermal stresses and intrinsic stresses.

Thermal stresses arise from differences in thermal expansion coefficients between coating and substrate: during final cooling

Table 3
Process parameters for PVD deposition

	Pressure (Pa)	Deposition t emperature (°C)	Bias (V)	Current (A)
PVD CrN coating	1.5	350	80 V	70
PVD TiN coating	2	450	150 V	70

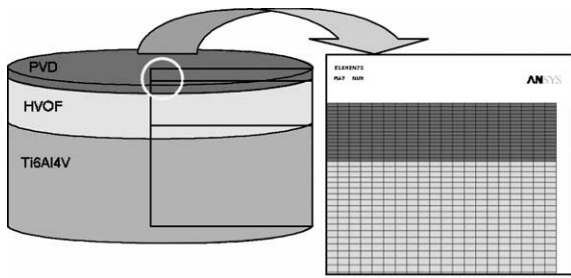


Fig. 1. Finite element model realized to evaluate residual stresses arising from the deposition processes.

from deposition to room temperature a misfit strain ε arises, leading to a residual stress given by the following equation:

$$\sigma_{th} = \left(\frac{E_f}{1 - \nu_f} \right) \cdot \varepsilon = \left(\frac{E_f}{1 - \nu_f} \right) \cdot (\alpha_s - \alpha_f) \cdot (T_r - T_s) \quad (1)$$

Where E_f and E_s are Young's modulus and Poisson's ratio of the film, respectively; α_f and α_s are the thermal expansion coefficients of the substrate and film, respectively.

Intrinsic stresses arise during deposition, as a consequence of crystal growth: the major part of the models developed nowadays agrees about the dependence of the intrinsic stress on ionic and atomic flux during the deposition, and on the energy of the bombarding ions [5].

Usually the resulting residual stress field is approximately calculated by the sum of the two sources:

$$\sigma_{tot} = \sigma_i + \sigma_{th} \quad (2)$$

On the other hand, also residual stresses for HVOF coatings arise from two main sources [8–10]: the quenching stress [8,9], which arises from the instantaneous cooling of the impacting droplets, and thermal stresses, also due to differential thermal contractions.

Although complex interactions between coexisting residual stresses of various sources can be generally expected, a sufficiently reliable prediction model can be developed for qualitative stress estimation and preliminary process optimisation by adopting realistic simplification hypotheses.

Using the commercial software ANSYS9.0, the finite element model (axisymmetric elements) showed in Fig. 1 was

realized in order to obtain a qualitative evaluation of the residual stresses for the duplex coating under evaluation: the model consists of a plane disk, in which the interfaces between coatings were assumed as perfect, mechanical and thermal properties of materials were assumed as temperature dependent and plastic behaviour of the substrate was taken into account as well.

The model simulates the thermal history of both the HVOF deposition and the PVD: the code imposes the final cooling from deposition temperature and calculates the subsequent residual stress field.

The intrinsic stress for PVD and the quenching stress for PVD were assumed as initial stresses: the intrinsic PVD stress was calculated using the model proposed in Ref. [5], whereas the quenching stress was evaluated from Ref. [8]: a value of -3 GPa (typical for CA–PVD coatings) was imposed as intrinsic stress for the PVD coating, whereas a value of $+70$ MPa was adopted for the quenching stress of WC–Co HVOF coating.

(1) In the xy-plane residual stress, (2) in the z-plane (normal to the surface) residual stress and (3) xy-shear residual stress were calculated and analysed, and a parametric study of the influence of substrate hardness, Young modulus and coefficient of thermal expansion was carried out, obtaining applicable information about the optimal material matching which allow to minimize normal residual stresses. The model allows also to point out differences between samples with different HVOF coating thickness, as well as information about the influence of residual stress on interface toughness.

2.4. Morphological and mechanical characterization of coatings

Morphological and compositional characterization of coating surface and layer interfaces were performed using Optical Microscopy (OM), Scanning Electron Microscope coupled with Emission Dispersive Spectroscopy (SEM-EDS) and AFM techniques.

The adhesion between PVD coatings and HVOF substrate was evaluated by cross-section SEM analyses during inspection of coating microstructure on LN₂ fractured surfaces; as shown in Fig. 5, the technique allows also to measure the coating thickness and acquire information about grain size and crystals growth.

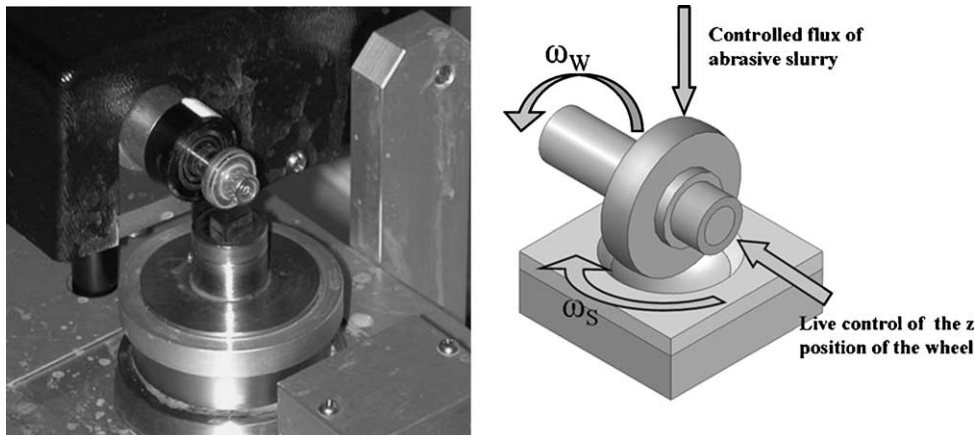


Fig. 2. Equipment developed for wear tests: variation in relative velocities allows to vary the abrading stress field.

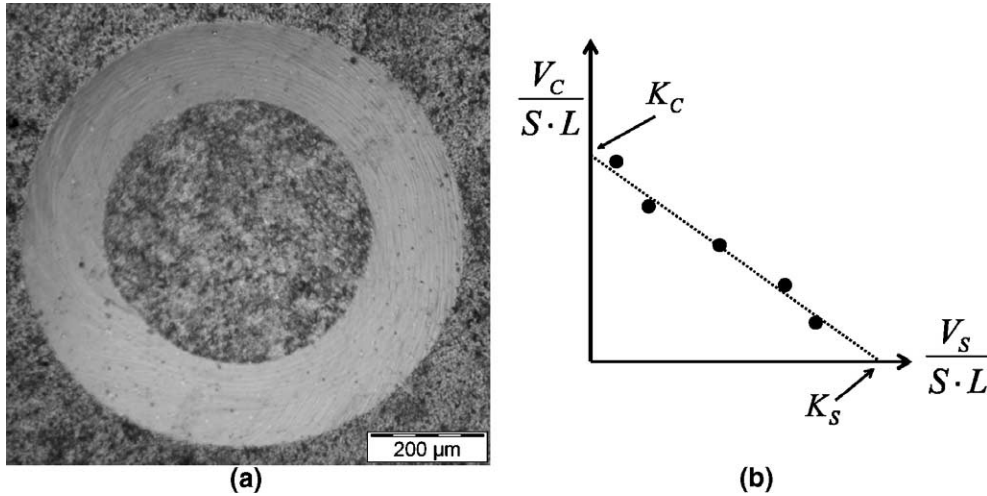


Fig. 3. (a) Typical wear crater obtained by the rotating wheel wear test (CrN on HVOF WC–Co duplex coating); (b) Procedure followed in order to calculate wear rates for coating and substrate (Archard Law).

The load carrying capacity of the coating was qualitatively evaluated using standard Rockwell C indentation test: by means of a standardized procedure [20], based on image analysis of fracture behaviour of the coating under a high load indentation test, it is possible to obtain information about coating toughness and adhesion, making an effective comparison between the PVD coatings on uncoated Ti–6Al–4V alloy and the duplex systems.

The Vickers hardness was measured by means of a microhardness tester, applying loads between 50 and 10,000 mN. The hardness was calculated by the diagonal length “d”. Depending on the applied load, the measure of “d” has been acquired: (1) directly on the hardness tester in the case of big indentation marks, or (2) both by SEM and AFM (NT-MDT Smena, contact mode, properly calibrated) in the case of indentation marks with lateral size below 3 μm. During the acquisition campaign, AFM measurements resulted to be more confident with respect to SEM, which depend on probe conditions, cleanness of sample surface and operator bias. The obtained value for each load corresponds to the mean of six measures. In order to extrapolate film hardness, the Jönsson–Hogmark and Chicot and Lesage models have been used [11,12]; since the HVOF coating is much thicker than the PVD ones, the influence of the Ti–6Al–4V substrate was assumed to be negligible for the in-plane microhardness tests.

Coatings resistance to abrasive wear was evaluated using a dimpling grinder equipment normally used to prepare TEM samples (Fig. 2), basing on the procedure exposed in literature [13–18].

The apparatus was equipped with a copper wheel, shaped as a disk cut out from the centre of a sphere. The grinding wheel

rotates around a horizontal axis (see Fig. 2), and the specimen, glued on a horizontal metal disk, rotates around a vertical axis. The combined motions result in a crater with a spherical cap shape being ground into the specimen: note that by increasing the angular velocity of the sample holder it is possible to increase the in-plane shear component of the abrading stress field with respect to the normal shear component, obtaining information about the possibility of coating delamination. In order to obtain reproducible results, runs are performed controlling the following parameters: flux of diamond abrasive slurry, applied load, speed and relative sliding distance.

In order to obtain the coatings intrinsic wear coefficient the Archard model [21] was used:

$$\frac{V_c}{k_c} + \frac{V_s}{k_s} = S \cdot L \tag{3}$$

where the mean applied load is assumed to be distributed over substrate and coating. Rearranging Eq. (3):

$$\frac{1}{k_c} \cdot \frac{V_s}{S \cdot L} + \frac{1}{k_s} \cdot \frac{V_c}{S \cdot L} = 1 \tag{4}$$

Wear coefficients of coating (K_c) and substrate (K_s) are calculated after experimental determination of abraded volumes,

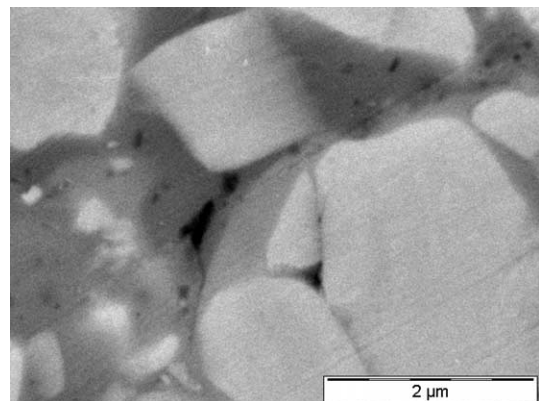


Fig. 4. Detail (SEM 20 kV BSE) of the polished HVOF surface: R_a , meas. by profilometer was 0.0157 μm.

Table 4
Parameters adopted for all the abrasive wear test performed

Load applied (N)	Abrading particles size (μm)	Sliding distances (m)	Angular velocity of rotating wheel (rpm)	Angular velocity of sample stage (low/high)
0.85	1	15, 18, 28, 38, 48	200	29/65

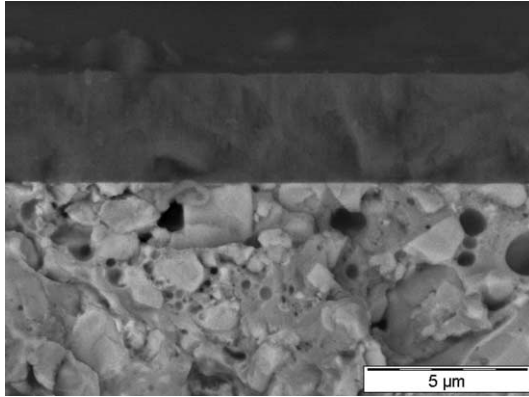


Fig. 5. LN2 fracture surface of CrN coating on WC–Co; no cracks are visible at the interface (20 kV, SE).

by linear fitting Eq. (6), as intercepts with V_c/SL and V_s/SL axes, respectively (Fig. 3): tests parameters are shown in Table 4.

Note that two levels of angular velocity of the stage were adopted, in order to evaluate the resistance of the coatings to failure under higher shear component of the stress [19].

3. Results

The optimized polishing procedures for HVOF coatings lead to the following results: the surface roughness R_a of the coating, measured by stylus profilometer, resulted to be $0.0157 \pm 0.0013 \mu\text{m}$, and no damage on the surface was noticed, as shown in Fig. 4.

On the other hand, this optimized polishing procedure resulted to be more expensive and complex than the traditional one.

The CrN coating obtained after PVD deposition is shown in Fig. 5: measured thicknesses were $3.4 \mu\text{m}$ for the CrN coating and $3.2 \mu\text{m}$ for the TiN one.

3.1. Analytical calculation of contact stress field

The critical load calculation performed for the systems under examination lead to the results shown in Fig. 6. It is important to notice that for a monolayer PVD coating on Ti–6Al–4V the increase in load bearing capacity is quite low compared to that one obtained for the duplex system: for high contact radii, the behaviour of the monolayer coating is predicted to be even worse than the uncoated Ti alloy.

A further result is obtained by plotting the contact stress distribution in both cases: considering the case of the hard PVD coatings on the much softer Ti alloy, a really high stress peak appears at interface (Fig. 7a).

The interposition of the stiffer and harder WC–Co interlayer involves a drastic reduction of that peak, which does not appear anymore in Fig. 7b.

So the duplex coating is expected to have a better adhesion, and to be much stronger and tough than the monolayer PVD coating: this fact was confirmed by the SEM investigation of the interfaces, and image analysis of the high load indentations, as explained in the following sections.

3.2. Finite element simulation of residual stresses

Results of finite element calculation of residual stresses are summarized in Table 5.

The model predicts high normal to the surface and shear interfacial stresses in correspondence of the sample edge for the

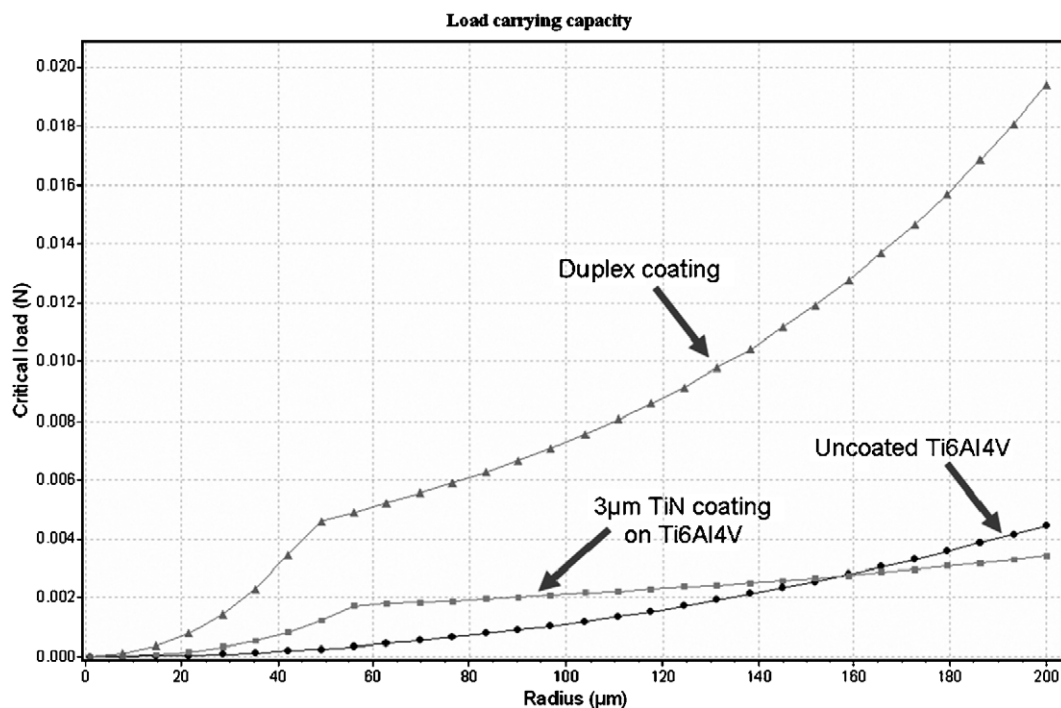


Fig. 6. Load bearing capacity of the uncoated, only PVD coated, and HVOF–PVD coated systems, obtained by analytical calculation of contact stress field.

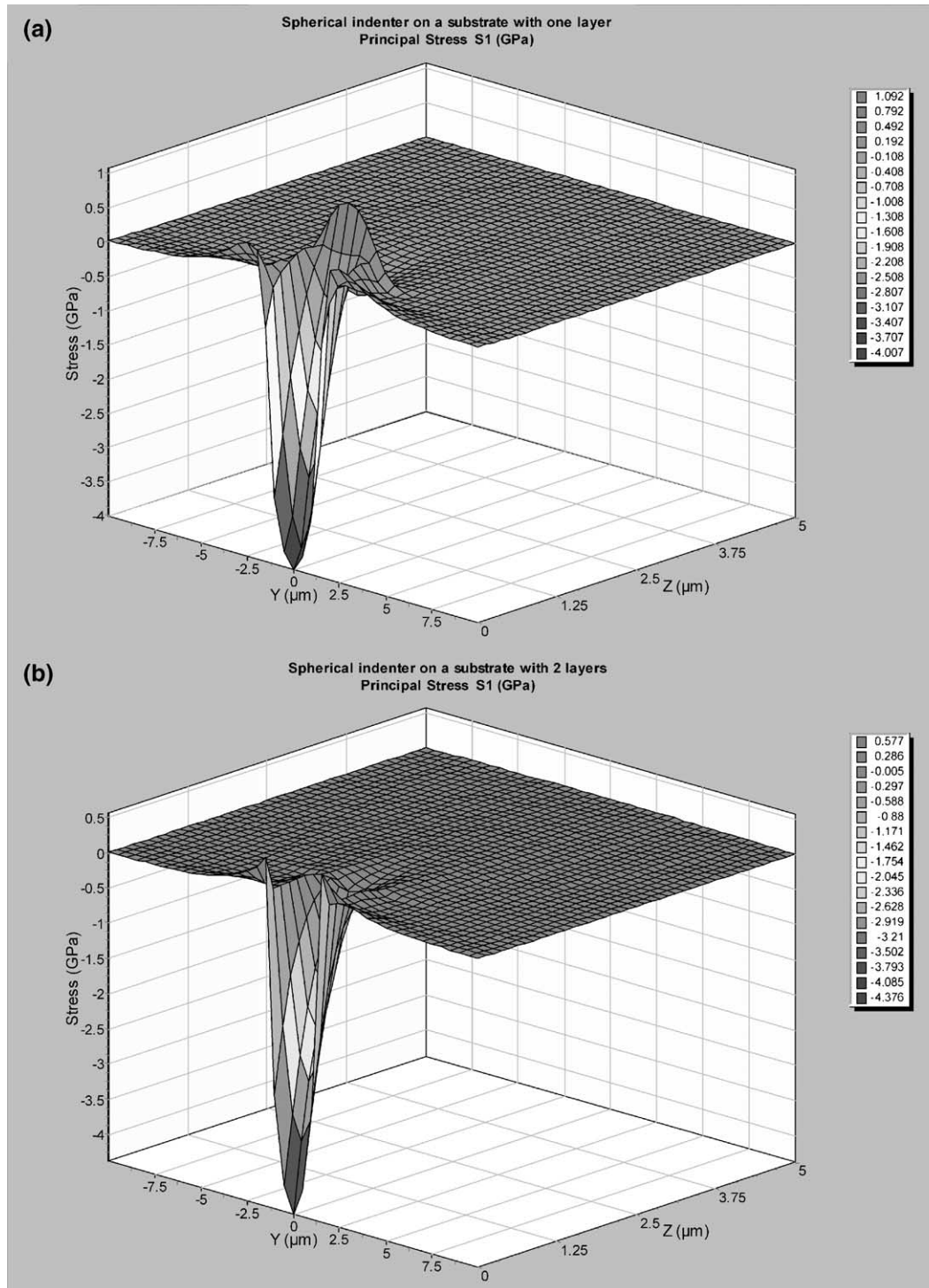


Fig. 7. (a) Stresses distribution (1st principal) for the contact with a spherical rigid body ($R=50\ \mu\text{m}$, $F=0.1\ \text{N}$): for the monolayer PVD coating a high interfacial stress peak is predicted; (b) contact stresses distribution (1st principal) under contact by a spherical rigid body ($R=50\ \mu\text{m}$, $F=0.1\ \text{N}$): in the case of the duplex systems under examination the interface stress peak disappears.

PVD coatings on uncoated Ti Alloy: this is likely due to the high differences in yield strength, elastic modulus and thermal expansion between the two materials.

Simulations performed for the duplex systems under examination predicted lower interfacial residual stresses compared to the ones calculated for the monolayer systems, most likely due to the

higher stiffness and hardness of the WC–Co interlayer, but also to its thermal properties: WC–Co shows values of thermal expansion coefficient which are intermediate between Ti–6Al–4V and the PVD coatings, involving a high reduction in thermal stresses.

Reduction in interfacial stresses was quantified as 30%, compared to the corresponding monolayer coating.

Table 5
Predicted residual stresses (FE model)

	Superficial in plane residual stress (MPa)	Maximum normal stress (MPa)	Interface shear stress (MPa)	Interface von Mises equivalent stress (MPa)
3 μm TiN on Ti–6Al–4V substrate	–2700	513	347	790
Duplex system (HVOF+3 μm TiN on Ti–6Al–4V substrate)	–2240	369	245	562 (reduction \approx 30%)
3 μm CrN on Ti–6Al–4V substrate	–3600	653	437	999
Duplex system (HVOF+3 μm CrN on Ti–6Al–4V substrate)	–3290	470	348	764 (reduction \approx 30%)

3.3. Morphological and mechanical characterization of coatings

No interfacial cracks were found during SEM cross-section analysis of the LN_2 fractured surfaces (Fig. 5): both coatings showed a very good adhesion on the WC–Co substrate.

In addition to this, also the HRC indent analysis lead to similar results: the duplex coating do not appear damaged at all, especially if compared to the monolayer one (see Fig. 8), where it appears completely damaged.

Vickers Hardness measurement and modelling lead to the results shown in Figs. 9, 10 and Table 6: the intrinsic mean value of microhardness for both the PVD coating are high and in good agreement with the values available in literature.

The most noticeable aspect is that the composite hardness of the duplex systems resulted to be very high as well, especially if compared with that one of the monolayer PVD system (see Table 6).

The implemented wear test described before, lead to the results illustrated in Table 6 and Figs. 11, 12; strictly controlling the slurry flux, made the procedure highly reproducible, so that only four tests at different sliding distances were usually enough to have a satisfactory fit between the Archard model and the experimental data (see Figs. 11, 12 for both CrN and TiN coatings).

The coated system shows a very good behaviour also in the case of high shear stress (see Table 6); in this case the wear coefficient does not decrease after increasing the sample stage velocity: other coated systems often showed failure under these severe conditions, as explained in a previous work [19].

4. Discussion

The duplex coating under examination showed good adhesion, high toughness and high load carrying capacity.

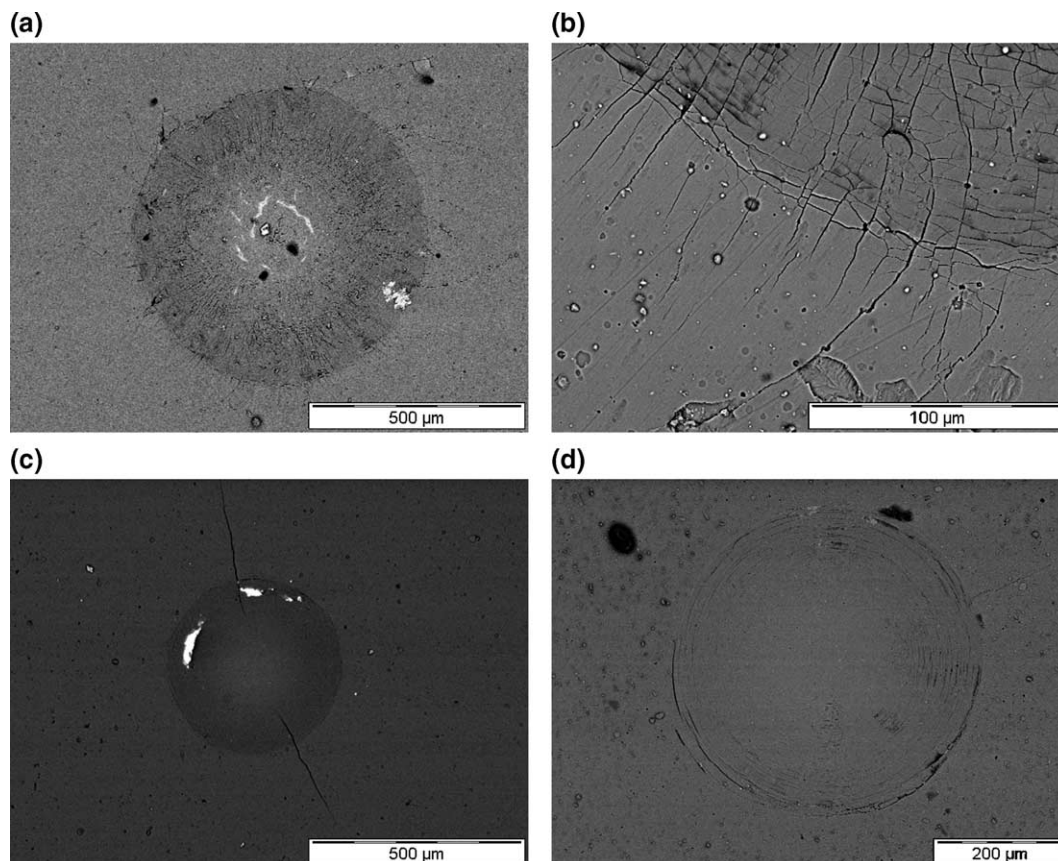


Fig. 8. Toughness and load bearing capacity evaluation by image analysis of HRC indentations: (a) TiN on uncoated Ti–6Al–4V (i.e., without HVOF–WC–Co); (b) detail of TiN on uncoated Ti–6Al–4V; (c) duplex TiN WC–Co, (d) duplex CrN WC–Co.

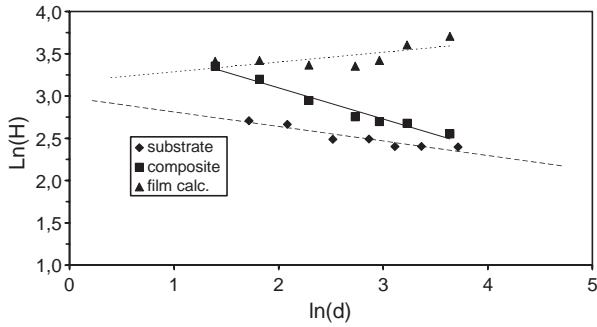


Fig. 9. Hardness modelling of the CrN WC–Co duplex coating (model of Chicot and Lesage [12]).

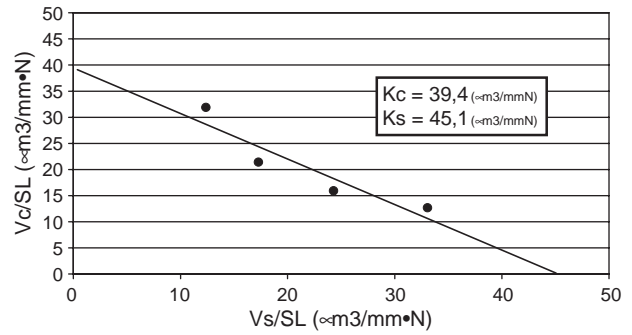


Fig. 11. Calculation of specific wear rates by interpolation of experimental data (CrN coating).

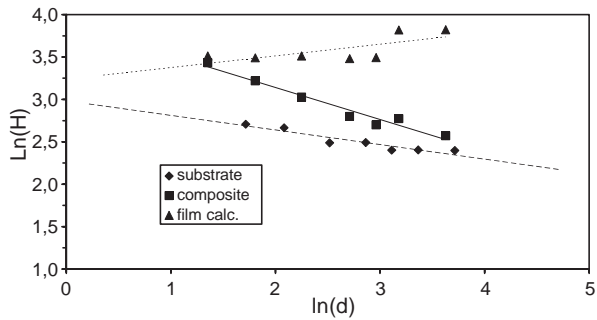


Fig. 10. Hardness modelling of the TiN WC–Co duplex coating (model of Chicot and Lesage [12]).

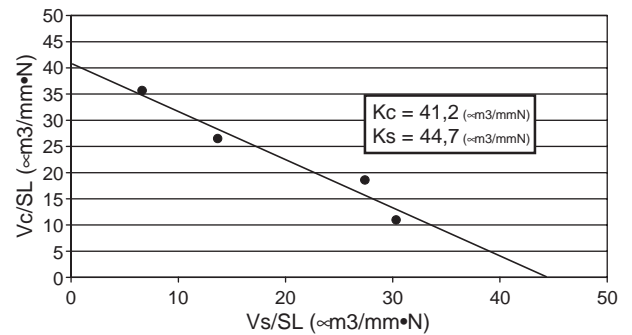


Fig. 12. Calculation of specific wear rates by interpolation of experimental data (TiN coating).

Considering the simulations performed, such a behaviour can be explained in terms of better material matching: the interposition of the harder, but also stiffer, HVOF interlayer involves a significant redistribution of the contact stress field, avoiding interfacial stress peak (see Figs. 6, 7).

The duplex systems commercially adopted (PVD coating on a nitrided interlayer) interpose only a harder but not stiffer interlayer, giving just a partial increasing in load bearing capacity.

From the point of view of residual stress, a higher and thermally stiffer (i.e., with lower thermal contraction coefficient) interlayer, surely contributes more to the reduction of thermal stresses (Table 5).

Finite element simulation also predicts a non-linear interaction between intrinsic stresses and thermal stresses: the code imposes the first ones as initial stresses, after which it imposes the thermal history of the deposition processes: results show that the two sources are not simply additvable (as usually proposed): it is likely that plastic relaxation during deposition

and final cooling involve a lower final value of in-plane residual stress.

The behaviour predicted by the simulations was confirmed by the experimental evaluation of toughness and adhesion: the system seems to be tough, even more than the PVD coating on tool steel commercially available [19].

The good adhesion between PVD coatings and substrate is not only due to the intrinsic properties of each material, but also to the surface preparation of the HVOF layer before PVD deposition: the optimized procedure developed (using diamond lapping films, Table 2) allowed to obtain the low roughness expected without coating damage.

In the case of the TiN WC–Co duplex system few radial cracks appear after Rockwell C indentation (always less than three, Fig. 8(c)): literature [20] suggests that a few number of radial cracks (lower than five) is evidence of good adhesion and toughness, whereas the presence of both ramified cracks and lakes of delamination means low adhesion (see Fig. 8(a)–(b)).

Table 6
Results summary for the mechanical and tribological characterization of the coatings

	Wear coefficient K_C ($\mu\text{m}^3/\text{mm}\cdot\text{N}$)	Behaviour at high shear abrading stresses	Intrinsic hardness of the PVD coating (Chicot model [12]) (GPa)	Adhesion (HRC and cross-section SEM observation)	Mean composite hardness (GPa)
TiN WC–Co	41.2 (substrate 44.7)	No coating failure	33.5	Class 1 (German standard: DIN CEN/TS 1071-8)	25.0
CrN WC–Co	39.4 (substrate 45.1)	No coating failure	30.3	Class 1	24.4
Only HVOF WC–Co	68.2	No coating failure	–	–	13.7
Only TiN PVD	45.1	No coating failure	27	Class 5	9

Comparing wear rate values obtained for studied system (composite wear rate $\approx 40 \mu\text{m}^3/\text{mmN}$, Figs. 11, 12) with wear rates normally obtained on tool steel ($100 \mu\text{m}^3/\text{mmN}$, measured by the same technique, [19]) such system results particularly favor those applications where resistance to severe wear and high concentrated loads, together with low weight, are needed (i.e., aeronautic and competition automotive applications).

The whole coating costs are obviously higher than a traditional duplex process (nitriding plus PVD) and also applicable for very limited component geometry (due to the careful polishing step); nevertheless the increase in the lifetime of the component could overcome its production costs for some specific applications.

The next step of this work will be a parametric study of the influence of HVOF coating thickness on mechanical properties of the system, aimed to determine the optimum thickness of each layer.

5. Conclusions

- The optimized HVOF polishing procedure has been the key point in guarantee a good adhesion between coatings: the procedure is reproducible, quick, but could be difficult to be scaled up to complex geometry (i.e., not plane or cylindrical).
- Analytical and finite element simulations indicate that the interposition of the WC–Co thick layer plays a critical role in increasing the load bearing capacity and the adhesion;
- The procedure resulted to be more expensive than the traditional Duplex ones and less versatile, but the coatings produced showed very high composite properties: high hardness, high toughness, good adhesion and low wear rate

(the wear test developed, implemented rotating wheel technique, allowed the obtainment of reproducible results);

- The coated system analysed can be particularly utilized for extreme mechanical applications.

References

- [1] T. Bell, H. Dong, Y. Sun, *Tribol. Int.* 31 (1998) 127.
- [2] E.O. Ezugwu, Z.M. Wang, *J. Mater. Process. Technol.* 68 (1997) 262.
- [3] G.W. Critchlow, D.M. Brewis, *Int. J. Adhes. Adhes.* 15 (1996) 161.
- [4] ELASTICA2.1, ESAE-Design, www.esae.de.
- [5] Y. Pauleau, *Vacuum* 61 (2001) 17.
- [6] G. Knuyt, W. Lauwerens, L.M. Stals, *Thin Solid Films* 370 (2000) 232.
- [7] V. Teixeira, *Thin Solid Films* 392 (2001) 276.
- [8] J. Stokes, L. Looney, *Surf. Coat. Technol.* 177–178 (2004) 18.
- [9] S. Kuroda, T.W. Clyne, *Thin Solid Films* 200 (1) (1991) 49.
- [10] T.W. Clyne, S.C. Gill, *J. Therm. Spray Technol.* 5 (4) (1996) 401.
- [11] O. Vingsbo, S. Hogmark, B. Jönsson, A. Ingemarson, *Mater. Sci. Eng. ASTM STP* 889 (1986) 257.
- [12] D. Chicot, J. Lesage, *Thin Solid Films* 245 (1995) 123.
- [13] R. Gahlin, M. Larsson, P. Hedenqvist, S. Jacobson, S. Hogmark, *Surf. Coat. Technol.* 90 (1997) 107.
- [14] P.H. Shipway, I.M. Hutchings, *Surf. Coat. Technol.* 71 (1995) 1.
- [15] M.G. Gee, A. Gant, I. Hutchings, R. Bethke, K. Schiffman, K. van Acker, S. Poulat, Y. Gachon, J. von Stebut, *Wear* 255 (2003) 1.
- [16] D.N. Allsop, R.I. Trezona, I.M. Hutchings, *Tribol. Lett.* 5 (1998) 259.
- [17] R.I. Trezona, I. Hutchings, *Wear* 233 (1999) 209.
- [18] Y. Kusano, K. Van Acker, I.M. Hutchings, *Surf. Coat. Technol.* 183 (2004) 312.
- [19] E. Bemporad, D. De Felicis, M. Sebastiani, T. Valente, F. Carassiti, *Proceedings of the VI Eur. Conf. of Vacuum Coaters, Anzio, Rome, September 2004*.
- [20] German standard DIN CEN/TS 1071-8.
- [21] J.F. Archard, *J. Appl. Phys.* 24 (1953) 981.
- [22] A. Bloyce, P.H. Morton, T. Bell, *Surface Engineering of Titanium and Titanium Alloys, Metals Handbook, vol. 5, ASM, 1994, Surface Engineering*.